ROYAL SOCIETY OF CHEMISTRY

Check for updates

Advanced mechanisms and applications of microwave-assisted synthesis of carbon-based materials: a brief review

Zhaolong Li, [ID] [abc] Kaiming Peng, [cd] Nannan Ji, [c] Wenlong Zhang, [ce] Wenrou Tian [c] and Zhenfei Gao*[c]

The interaction of microwave radiation with carbon-based materials induces rapid, instantaneous heating. When combined with the plasma excitation capabilities of microwaves, this property presents novel avenues for synthesizing carbon-based materials that require high temperatures and catalytic activity. This review investigates the response of carbon-based materials to microwave radiation, analyzes the dielectric loss mechanism responsible for heat generation, and details the microwave plasma excitation mechanisms employed in the synthesis and processing of carbon-based materials. Furthermore, the structure of microwave reactors is discussed, followed by a discussion of their diverse applications in both laboratory and industrial settings. Lastly, the review addresses the challenges associated with the practical implementation of microwave technology and explores future development prospects, with a particular focus on the application of microwaves in carbon-based material synthesis.

1. Introduction

Carbon-based materials, such as graphene, carbon nanotubes, and graphdiyne, consist of carbon atoms arranged in specialized structures and play a crucial role in various domains, including electronic devices,[1] energy storage,[2] catalysis,[3] biomedicine,[4] and environmental protection,[5] due to their exceptional electrical conductivity, mechanical strength, and thermal properties.[6] High-temperature reactions are commonly employed in the production of carbon-based materials, typically involving complex processes with low energy conversion efficiency. These methods require a significant amount of electricity or fuel, leading to increased carbon emissions and energy consumption. To tackle the challenges of energy constraints and greenhouse gas emissions, the concept of carbon neutrality has gained considerable attention in scientific research and technological innovation.[7] Consequently, the development of rapid, eco-friendly, and cost-effective heat treatment processes has emerged as a major research focus in recent years.

Microwaves in the electromagnetic spectrum, ranging from 0.3 GHz (wavelength: 1 meter) to 300 GHz (wavelength: 1 millimeter), can be divided into ultra-high frequency (300 MHz to 3 GHz), super high frequency (3–30 GHz), and extremely high frequency (30–300 GHz).[8] The discovery of the thermal effects of microwaves by the U.S. Raytheon Company in 1945, which led to the introduction of the world's first commercial microwave oven, the Radarange, paved the way for the application of microwave technology in various fields.[9]

As shown in Fig. 1, most carbon-based materials can undergo various interactions in the presence of microwaves due to their unique electronic structure (closely linked or overlapping conduction and valence bands) and delocalized π-electrons. This characteristic makes them effective as heating media, precursors, and reaction hotspots for composite materials.[10–13] In order to adapt to the different reaction conditions, various types of microwave reactors have been developed. For example, minor modifications to domestic microwave ovens allow for the synthesis of catalytic carbon-based materials. Microwaves can be utilized in the preparation of carbon nanostructures from rice husks,[14] and microwave-excited plasma can be employed for the one-step synthesis of carbon nanomaterials.[15] Additionally, microwave reactors are being developed and improved for industrial production,[16] effectively reducing energy consumption and carbon emissions compared to traditional high-temperature furnaces.[17,18] Microwave reactions have the advantages of rapid instantaneous heating, which reduces processing time,[19] facilitates catalytic reactions,[20] reduces side reactions,[21] and enables new reaction pathways.[22] The number of publications

[a]State Key Laboratory of High-efficiency Coal Utilization and Green Chemical Engineering, College of Chemistry and Chemical Engineering, Ningxia University, Yinchuan, 750021, China

[b]School of Materials Science and Engineering, Beijing Science and Engineering Center for Nanocarbons, Peking University, Beijing, 100871, China

[c]Beijing Graphene Institute, Beijing, 100095, China. E-mail: gaozf-cnc@pku.edu.cn

[d]Academy for Advanced Interdisciplinary Research, North University of China, Taiyuan, 030051, China

[e]State Key Laboratory of Heavy Oil Processing, China University of Petroleum, Beijing, 102249, China
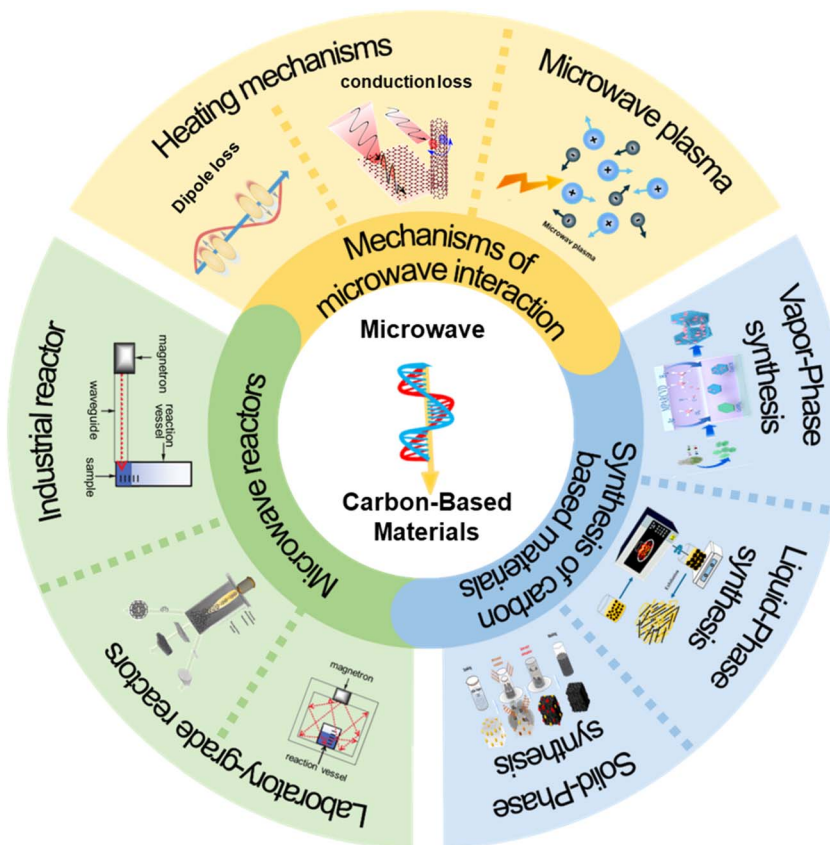
Fig. 1 Scheme of microwave reaction mechanisms in the production of carbon-based materials, microwave reactors and preparation.

on carbon-based materials and microwaves has continuously increased over the past 20 years (Fig. 2), demonstrating the rapid development and application of microwave technology in the field of carbon-based materials preparation.

This review aims to describe the reaction mechanisms between microwaves and carbon-based materials, thoroughly examine the microwave reactor, and introduce the application of microwave technology in the preparation of carbon-based materials. Section 1 discusses the main principles and factors affecting the microwave preparation process, while Section 2 describes the microwave reactor and compares experimental

and industrial reactors. Given the diverse experimental processes available for microwave preparation, modification, and the creation of composite materials, as well as the impressive research results published to date, Section 3 highlights some typical articles to illustrate the wide applicability of microwaves. Finally, we review the challenges and prospects of microwave applications in this field, aiming to broaden the development and application of microwave technology and reactors in the preparation of carbon-based materials. By analyzing the current research results and looking forward to future challenges, this review provides a strong reference and guidance for the further development of microwave technology and reactors in the field of carbon-based materials.
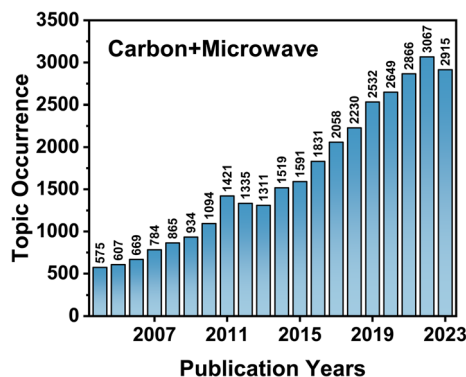
2. Mechanisms of microwave interaction

Electromagnetic waves interact with materials in three different modes: refraction, reflection, and absorption.[23–25] The same applies to microwave reactions, and these modes can occur individually or in combination. In the heating of carbon-based materials, absorption is the primary mechanism of microwave radiation interaction. However, reflected and unabsorbed waves can cause irreversible damage to the magnetron that generates microwaves.[26]

Microwave absorption in carbon-based materials is known as microwave loss, in which the electric and magnetic fields of

Fig. 2 Topic carbon and microwave occurrences from 2004 to 2023 in the Web of Science.

© 2025 The Author(s). Published by the Royal Society of Chemistry

microwaves force dipoles, free electrons, or magnetic domains to align with the oscillating field. Due to the rapid changes in the field, dipoles cannot fully synchronize, leading to molecular friction and collisions, which convert microwave energy into heat. Similarly, free electrons are agitated by the oscillating electric field, resulting in resistive heating, while magnetic domains experience losses due to the reorientation of magnetic moments under the influence of the magnetic field. These effects raise the material's temperature.[27,28] Microwave losses are classified into dielectric and magnetic losses, such as dipole losses, conduction losses, hysteresis losses, eddy current losses, *etc.*[29–31] Unlike traditional thermal radiation methods, microwave heating generates heat directly within the material, bypassing any interaction with the surrounding environment, resulting in direct heating and achieving a more uniform heat treatment effect (Fig. 3).

2.1 Microwave heating mechanism

When the microwave interacts with the absorbing material, dipole molecules and ions are driven to friction, collision, and movement by the alternating electric field. This interaction gives rise to dipole polarization and interface polarization, both of which correspond to rearranged motion. The polarization time of both types coincides with the microwave frequency range of 10^{-9} to 10^{-12} seconds, ultimately resulting in the dissipation of energy from collisions and motion as heat.[32] In an electric field, the polarization of carbon-based materials manifests as a loss of current density to the electric field, measured using the complex dielectric constant ε^*:

$$\varepsilon^* = \varepsilon' - j\varepsilon'' \tag{1}$$

where j is the imaginary unit, ε' is the relative dielectric constant, which is related to the ability of molecules to polarize in an electric field and indicating the material's capacity to store electrical energy, and ε'' is the relative dielectric loss factor, indicating the material's ability to dissipate electrical energy as heat.[33–35]

The dielectric loss tangent angle ($\tan(\delta)$) allows for comparison of the rate of warming of materials with similar chemical or physical properties when heated by an electric field:

$$\tan(\delta) = \frac{\varepsilon''}{\varepsilon'} \tag{2}$$

Using the Debye model,[36–38] it is also possible to compute the complex permittivity of a dielectric material with a single relaxation time constant as a function of microwave frequency:

$$\varepsilon^* = \varepsilon_\infty + \frac{\varepsilon'_s - \varepsilon'_\infty}{1 + j\omega\tau} \tag{3}$$

where ω is the angular frequency, τ is the relaxation time, which indicates the time (usually a few nanoseconds) when the molecular orientation remains unchanged after the microwave stops excitation, ε_s is the static permittivity, and ε_∞ is the high-frequency permittivity, which corresponds to the frequencies $\ll\tau^{-1}$ and $\geq\tau^{-1}$, respectively. It is also possible to separately derive the expressions for the frequency dependence of the permittivity and dissipation factor:

$$\varepsilon'_d = \varepsilon'_\infty + \frac{\left(\varepsilon'_s - \varepsilon'_\infty\right)}{1 + \omega^2\tau^2} \tag{4}$$

$$\varepsilon''_d = \frac{\left(\varepsilon'_s - \varepsilon'_\infty\right)\omega\tau}{\left(1 + \omega^2\tau^2\right)} \tag{5}$$

When the dielectric loss reaches its maximum value, the dielectric loss factor in the Debye equation and the relaxation time become independent of the high frequency:

$$\varepsilon''_{max} = \frac{\left(\varepsilon'_s - \varepsilon'_\infty\right)}{2} \tag{6}$$

Conduction loss also occurs in electrically conductive carbon-based materials.[39] When exposed to microwave radiation, internal free charge carriers move back and forth along the direction of the applied microwave electric field, generating current. Due to the induced magnetic field, the movement of electrons is influenced by inertia, elastic collisions and molecular interactions, resulting in friction and uniform heating of the material.[40] Conduction loss accounts for the effect of the individual conducting regions within the material, and its complex dielectric constant can be expressed as:

$$\varepsilon_c^* = \varepsilon'_\infty + \frac{\left(\varepsilon'_s - \varepsilon'_\infty\right)}{\left(1 + j\omega t\right)} - \frac{j\sigma}{\omega\varepsilon_0} \tag{7}$$
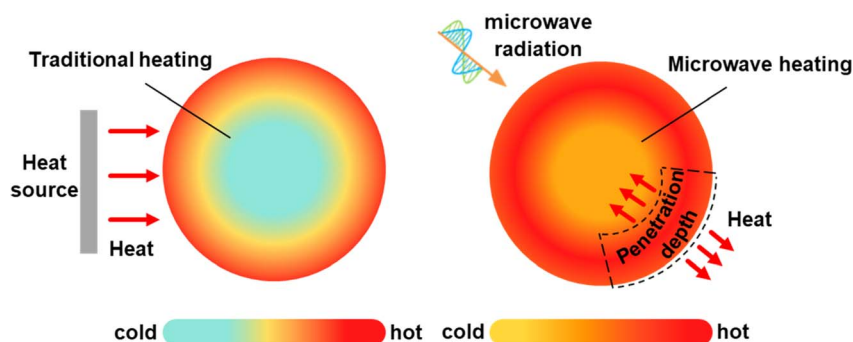

Fig. 3 Different heating models for conventional and microwave heating.

where ε_0 is the permittivity of free space, valued at 8.85×10^{-12} F m^{-1}.

The dielectric constant follows the same expression as that in the Debye equation, but the dielectric loss factor exhibits a relaxation response due to the induced current. In composites with higher conductivity, the conduction loss generated by microwaves may surpass the dipole loss.

Once the microwave field strength, frequency, and complex dielectric constant of the material are determined, the average absorbed power of the material, expressed in terms of the Debye parameter, can be calculated as:

$$P = \frac{\varepsilon_0 \left(\varepsilon'_s - \varepsilon'_\infty \right) \omega^2 \tau}{1 + \omega^2 \tau^2} |E|^2 \tag{8}$$

where E is the electric field strength of the microwave. In reality, the local field strength of the microwave is determined by the input power, the shape and size of the waveguide cavity, and the complex dielectric properties of the material itself.[32,41,42]

Hysteresis and eddy current losses are primarily associated with microwave magnetic fields and typically occur in magnetic conductors or semiconductors. During the microwave reaction process, rapid changes in the external magnetic field cause magnetic domain resonance and hysteresis within the material. Additionally, changes in the magnetic field generate closed-loop eddy currents that resist these changes, both of which generate heat. These effects are represented by complex permeability:

$$\mu = \mu' - j\mu'' \tag{9}$$

Similar to dielectric loss, μ' is the relative magnetic constant, measuring a material's ability to store magnetic energy, while μ'' is the relative magnetic loss, measuring a material's ability to convert magnetic field energy into heat.

Carbon-based materials are not inherently magnetic, but doping or synthesizing carbon based materials can introduce magnetic losses.[43,44] For example, compositing carbon with a ferromagnetic material can result in higher hysteresis losses.[45] The effective magnetic loss (μ''_{eff}) of a carbon matrix composite consists of hysteresis losses, eddy current losses, and other magnetic losses:

$$\mu''_{eff} = \mu''_{hysteresis} + \mu''_{eddycurrent} + \mu''_{residual} \tag{10}$$

The effect of penetration depth must also be considered in microwave reactions. Penetration depth refers to the depth at which the microwave intensity decreases to $1/e$ (approximately 37%) of its original intensity.[46] For carbon-based materials with high dielectric loss and low magnetic loss characteristics, the penetration depth using the Debye parameter can be expressed as:

$$D_p = \frac{\sqrt{2}C}{\omega \left\{ \left(\varepsilon_\infty + \frac{\varepsilon'_s - \varepsilon'_\infty}{1 + (\omega\tau)^2} \right) \left(\sqrt{1 + (\tan^2(\delta))^2} - 1 \right) \right\}^{\frac{1}{2}}} \tag{11}$$

where D_p is the penetration depth and C is the speed of light. Within a certain frequency range, the polarization behavior of materials and dielectric loss together determine the variation in

penetration depth.[47] As the frequency ω and the dielectric loss $\tan\delta$ increase, the polarization capability of the material is significantly enhanced. This change improves the absorption of electromagnetic waves, thereby leading to a reduction in penetration depth. Moreover, under high-frequency conditions, the polarization effect of the material is further enhanced, resulting in increased energy loss.[48] It should be noted that if the penetration depth is much smaller than the size of the material, only the surface of the incident wave will absorb the energy, leading to non-uniform heating.

2.2 Other effects of microwave

Microwaves can easily excite and produce plasma. Plasma consists of a large number of charged particles, forming a macroscopically neutral system in space. Like solids, liquids, and gases, plasma is a state of matter that exists at higher energy levels.[49]

When the root-mean-square value of the microwave electric field reaches the strength of the breakdown electric field, it causes the gas medium to undergo a breakdown process, leading to particle ionization and plasma excitation.[50] The functional expression for the breakdown electric field E_b is

$$E_b = E(U, L, Z, \lambda) \tag{12}$$

where U is the ionization potential of the gas molecules, L is the electron mean free path, Z is the characteristic diffusion length of the vessel, and λ is the wavelength of the microwave electric field.

At a fixed microwave frequency, the breakdown electric field of commonly used working gases, in descending order, is as follows: $H_2O > CO_2 > N_2 > O_2 > Ar > Ne$.[51] Inert gases are usually chosen as discharge gases to enhance plasma stability.[52] Since the theoretical breakdown electric field value of argon under standard atmospheric pressure is much lower than the strength of the atmospheric breakdown electric field, argon, which is also cost-effective, is often used as the working gas without considering other reaction conditions. Under low-pressure conditions, electrons and molecules have higher kinetic energy, making it easier to excite plasma.[53] In this case, the electron temperature (T_e) is lower than the gas temperature (T_g), indicating non-thermal equilibrium plasma. Specifically, when microwaves interact with carbon-based materials, the kinetic energy of certain small regions of π electrons extending outside the usual conjugated region can increase, transforming them into high-energy electrons. These high-energy electrons move rapidly across the surface of the carbon material, ionizing the surrounding reactive gas and creating high-temperature, arc-like micro-plasma hotspots. These hotspots help sustain and excite the chain reaction, resulting in strong plasma.

Plasma formed by ionizing gas using microwaves as an excitation source can result in a highly ionized and dissociated gas, yielding active particles. This plasma possesses a unique activation ability, enabling the growth of nanostructures without catalysts and creating favorable conditions for nucleation and growth processes. The energy density of a microwave plasma reactor is exceptionally high. By appropriately designing

the reactor and adjusting parameters such as microwave input power and gas pressure, the plasma can be used to dope and compound carbon-based materials through synergistic methods.[54,55]

3. Microwave reactor

Microwave reactions are widely utilized in both laboratory and industrial settings, leading to the development of various types of microwave reactors tailored to different applications and scales.[9,56,57] Whether for scientific research in laboratories or large-scale industrial production, all microwave reactors rely on a microwave energy transmission and control center. Despite their differences, these systems share many common features in their basic structure:

1. The use of the magnetron as a microwave generator: the magnetron is the core component of a microwave reactor, converting electrical energy into microwave energy through the interaction of electrons and a high-frequency electromagnetic field. Magnetrons can be categorized based on their operating state into pulse magnetrons and continuous-wave magnetrons; according to their structural characteristics, they can be divided into ordinary magnetrons, coaxial magnetrons, and anti-coaxial magnetrons; and based on whether the frequency is adjustable, they can be classified as fixed-frequency magnetrons or frequency-adjustable magnetrons.

2. Using a three-pin tuner for impedance matching: the equivalent circuit is modified by adjusting the length of the tuner's three pins inside the waveguide. This adjustment ensures that the combined impedance of the three-pin tuner and the load equals the characteristic impedance of the main transmission line, thereby minimizing microwave reflections and losses.

3. The reaction zone is a resonant cavity of specific size and shape. It ensures that transmission of microwaves is amplified and stabilized inside the cavity, based on the resonance phenomenon. The size and shape of the cavity are typically designed in conjunction with electric field simulations to achieve optimal field distribution.[58]

Based on these basic components, one can create single-mode microwave devices that excite a single electromagnetic mode, ensuring uniform heating and efficient energy transfer, which is suitable for precise laboratory experiments.[59] Conversely, multi-mode microwave devices excite multiple electromagnetic modes to cover a larger heating area, making them ideal for large-scale industrial production.[60]

3.1 Laboratory microwave reactor

The laboratory microwave reactor plays a crucial role in scientific research, providing researchers with an efficient and precise tool. Its application in chemical synthesis, material preparation, and material processing can significantly improve experimental efficiency, shorten the experimental cycle, and reduce costs.

The domestic microwave oven is the most commonly used experimental microwave reactor, primarily for preparation experiments that do not produce large quantities of gas. This is because such experiments typically either do not generate large quantities of gas or do not involve material expansion that could lead to pressure changes. The microwave power in these devices is operated by a magnetron that starts and stops periodically at specific time intervals, and the electrical structure is very simple. Bajpai et al.[61] achieved a 26% yield in the growth of carbon nanotubes (CNTs) within 5 minutes using a mixture of graphite, ferrocene, and carbon fiber precursors at 1800 W microwave power in a microwave oven at ambient temperature. This method does not require complex reactors or pretreatment processes, simplifying the CNT growth process and reducing production costs. Voiry et al.[62] used 1–2 second microwave pulses to rapidly reduce graphene oxide (Fig. 4a). The Raman spectrum of microwave-reduced graphene oxide exhibits characteristics similar to those of defect-free graphene, with sharp G and 2D peaks and almost no D peak, and most of the oxygen functional groups have been removed.

In addition, for mobile-phase continuous chemistry experiments or those with special requirements for pressure and atmosphere, the microwave reactor can be adapted.[63,64] This flexibility also allows for additional monitoring of temperature and auxiliary modules, meeting the needs of a variety of complex experiments.[65] The use of silicon carbide reaction vessels and fiber optic probes allows accurate monitoring of lower temperature ranges and helps control the progress of the reaction.[66] Gunnewiek et al.[67] used high microwave power combined with stirrer assistance to achieve rapid and uniform carbothermal reduction, preparing well-crystallized equiaxed boron carbide and a small amount of elongated nanoparticles with diameters of about 50 nm from reduced boric acid in 20 minutes (Fig. 4b).

Microwave Plasma Chemical Vapor Deposition (MPCVD) is another type of reactor widely used at the laboratory level for the synthesis and processing of carbon-based materials using microwave-excited plasma.[68–70] This reactor uses microwaves to create plasma and a highly reactive environment, which facilitates the decomposition of precursor gases and the deposition of materials. The MPCVD reactor essentially consists of a microwave generator, a circulating water load to absorb excess microwave power, a tuner for impedance matching, a waveguide for microwave transmission, a short-circuit piston to adjust the standing wave pattern, and an excitation cavity which can be either a rectangular waveguide with integrated quartz or ceramic tubes or a cylindrical metal resonant cavity (Fig. 4-c).Using a rectangular waveguide with an integrated quartz tube as the excitation chamber in MPCVD allows plasma to be excited over a wide pressure range, from low pressure to atmospheric pressure. Microwave plasma promotes the efficient decomposition of carbon and other doped precursors, providing gas temperatures up to 3000 K and producing a range of molecular and atomic species that can be assembled into graphene or other modified carbon-based materials.[71,72] Sun et al.[73] developed a "pulse-etched" microwave plasma process for scalable, high-purity graphene production, yielding small (≈ 180 nm), high-quality graphene with low oxygen content and a gas–solid conversion efficiency of $\approx 10.46\%$. Using
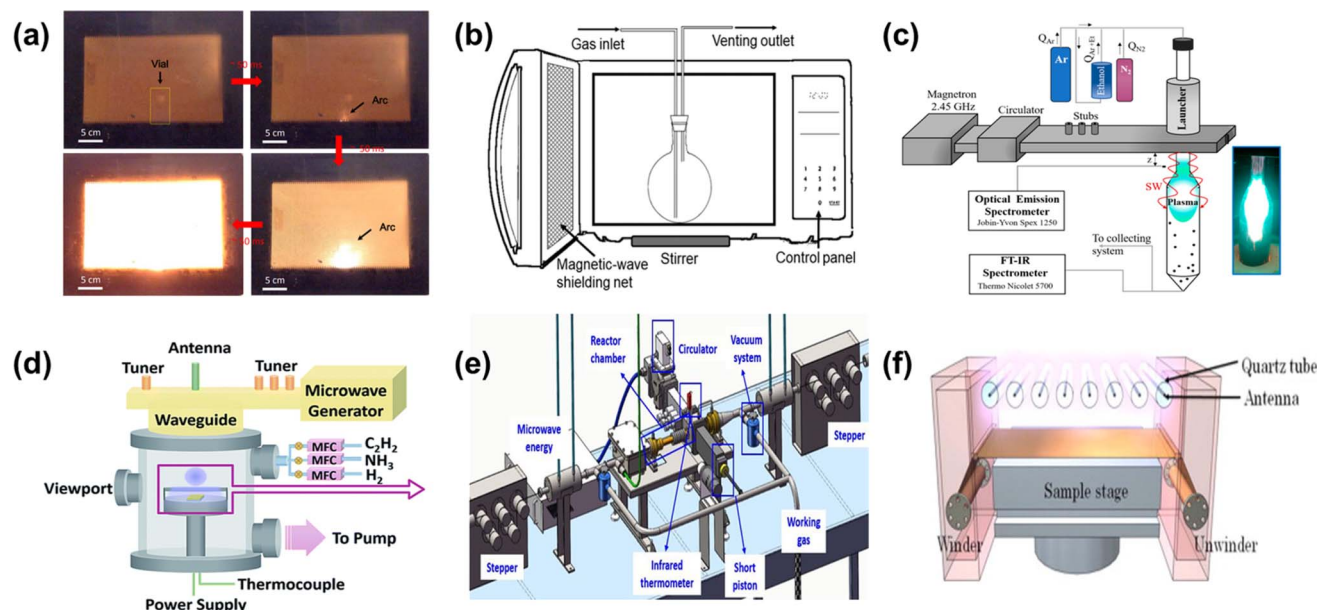
Fig. 4 Schematic diagram of various types of microwave reactors. (a) The domestic microwave oven. (b) Adapted domestic microwave oven. (c) Typical composition diagram of a MPCVD reactor. (d) MPCVD for large area reaction zone type. (e) Continuous microwave plasma reactor systems for the production of fibres. (f) Systems of a roll-to-roll microwave plasma reactor.

a cylindrical metal resonant cavity microwave in MPCVD to increase strong electric field coupling generates a spherical plasma (Fig. 4d). This type of plasma provides a low-temperature, large-area reaction zone during material preparation, which can be used to prepare diamonds[74] and graphene films,[75] as well as to perform large-area surface modification and cleaning of materials.[76,77]

Additionally, some systems combine conventional equipment with microwave reactors to achieve continuous material processing. Gao et al.,[78] for example, combined a carbon fiber winder with single-mode microwaves to achieve fast and efficient graphitization of carbon fibers, overcoming the drawbacks of conventional heat treatment processes (Fig. 4e). Yamada et al.[79] used a system combining roll-to-roll equipment and microwave surface wave plasma to deposit graphene films up to 294 mm wide on copper foil at temperatures below 400 °C, forming 3–4 layers of graphene in less than 100 seconds (Fig. 4f).

3.2 Industrial microwave reactor

Compared to laboratory microwave reactors, industrial microwave reactors are characterized by their ability to handle large-scale continuous material processing.[80] These systems typically have larger sizes, more complex combinations of components, and higher total output power.[81]

Mitsui Chemicals, Inc. and Microwave Chemical Co, Ltd.[82] established an innovative and environmentally friendly basic technology for carbon fiber recycling and production using microwave heating (Fig. 5a). This technology has been fully applied to the oxidation and carbonization processes, which are the most energy-intensive steps in carbon fiber production.[83] The use of microwaves reduces the size of the reactor, cuts

energy consumption by about 50%, and dramatically reduces process times compared to conventional preparation methods. 6K Inc.[84] in the USA has developed the UniMelt system, which features an atmospheric pressure microwave plasma generator as its core (Fig. 5b). This system allows for large-area production with uniform temperature distribution and achieves preparation results that surpass those obtained with arc electrodes or inductively coupled plasma. Furthermore, it enables the simultaneous preparation of nano- and micron-sized powders with improved control over particle size, purity, and morphology. The versatility of this microwave platform enables the production of various high-performance materials, such as lithium-ion battery materials, advanced coatings, and specialty ceramics. The high power microwave continuous processing system manufactured by AMTek[85] combines two sets of 915 MHz high-power microwave systems with a conveyor system of a push-plate furnace (Fig. 5c). Controlled by a PLC (Programmable Logic Controller), this system enables the continuous processing of materials such as the production of reduced graphene oxide, the sintering of ceramics, and the sterilization of pigments.

Industrial microwave reactors offer outstanding advantages in material preparation. Their large processing capacity and efficient energy management significantly improve production efficiency and environmental benefits, providing strong support for sustainable production across various industries.

4. Microwave-assisted synthesis of carbon-based materials

Based on the characteristics of microwaves, such as high efficiency, energy saving, flexibility, and strong adaptability,

Fig. 5 (a) Schematic diagram of the microwave reactor for the production of carbon fibres and its applied products. (b) The UniMelt system of 6K Inc. and its applied products. (c) The microwave continuous processing reactor of AMTek and its applied products.

microwave reactions are applied to the synthesis and modification of carbon-based materials, including zero-dimensional carbon quantum dots, one-dimensional carbon nanotubes, two-dimensional graphene, three-dimensional porous carbon, and other carbon-based materials. This section will discuss the application of microwave reactions in the preparation of carbon-based materials for gaseous,[86,87] liquid,[88,89] and solid[90,91] systems separately.

4.1   Microwaves in gaseous reactions

In chemical vapor synthesis reactions, microwaves have been utilized as an efficient enhancement method. Microwave chemical vapor synthesis effectively cracks the carbon source and synthesizes carbon-based nanomaterials by adjusting the gas source ratio, microwave processing power and time to control the process.

The importance of biomass as a renewable and clean energy source is multifaceted, as its utilization can reduce dependence on fossil fuels. Plasma technology offers an efficient method for biomass pyrolysis, with microwave plasma capable of producing carbon-based gas products with lower tar content and higher calorific value at lower temperatures compared to conventional biomass pyrolysis processes (Fig. 6a).[92]

At atmospheric pressure, microwaves can create a plasma region in the reactor that reaches temperatures of up to 4000 K, enabling rapid synthesis of self-supporting graphene sheets by introducing carbon sources such as methane or ethanol

(Fig. 6b). Tatarova et al.[93] selectively synthesized high quality graphene flakes, achieving yields of up to 2 mg min^{-1}, by tuning a high energy density plasma environment and using a combination of in situ infrared and ultraviolet radiation. The authors proposed a unique reaction mechanism using microwave plasma, in which carbon precursors are decomposed in the microwave plasma region to produce reactive species such as carbon atoms and C_2 radicals. These species are then transported out of the reactor to assemble and grow in a subsequent "mild" plasma region, enabling the sequential large-scale fabrication of self-supported graphene and N-doped graphene flakes (Fig. 6c).

Frenklach et al.[94] used an atmospheric pressure microwave plasma reactor for the gas-phase synthesis of graphene, synthesizing monolayer or bilayer graphene flakes without the need for three-dimensional materials or substrates by introducing droplets of liquid ethanol into an argon plasma. Raman spectroscopy and electron energy-loss spectroscopy (EELS) results confirmed the formation of graphene. This report demonstrates the feasibility of producing graphene sheets at the atomic scale in an atmospheric pressure microwave plasma reactor and suggests a potential route for the large-scale production of graphene. Zhang et al.[73] reported a "pulse etching" microwave-induced "snowfall" (PEMIS) process for the continuous and scalable preparation of high-quality, high-purity graphene directly in the gas phase. As shown in Fig. 6a, the graphene prepared by this method exhibits good thermal
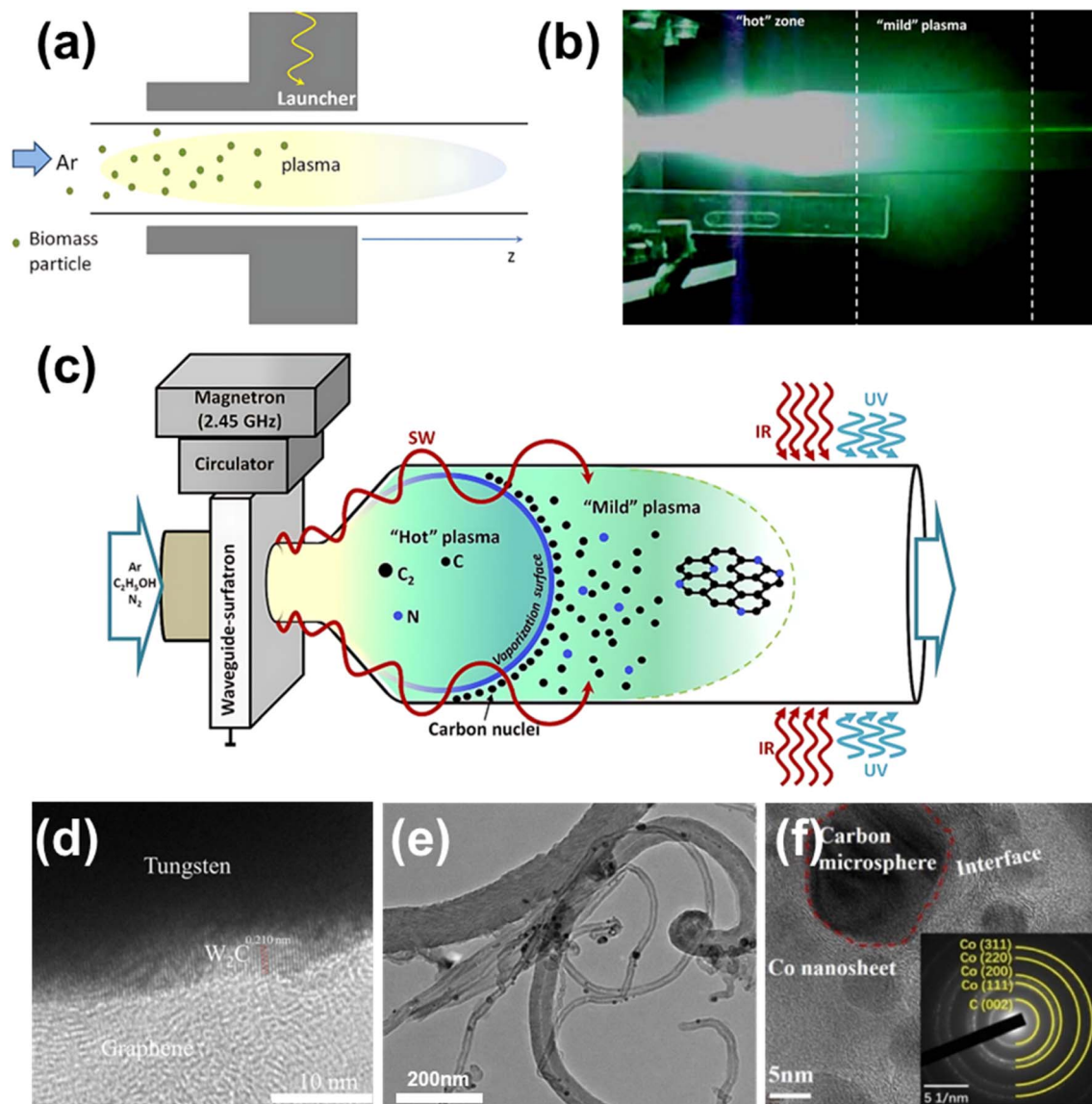
Fig. 6 (a) Plasma column with biomass particles. (b) The generated plasma torch. (c) Mechanism of growing graphene in atmospheric plasma. (d) HRTEM image of the interface of graphene and tungsten tip, (e) the TEM image of Ni–Pd-CNT and (f) Co@carbon microsphere.

conductivity and low defect density ($I_D/I_G \approx 0.27$). Gao et al.[95] utilized this process to prepare graphene with excellent mechanical properties for reinforcing the mechanical strength of meso-aramids.

Graphene composited with metals in gas-phase preparation by MPCVD can impart metal materials with excellent optical transparency, electromagnetic properties and catalytic properties, thereby expanding the application areas of traditional materials. Tang et al.[96] prepared graphene STM probes by growing graphene directly on tungsten needles using MPCVD. Atomic resolution TEM images revealed that the graphene flakes had good crystallinity with AB stacking (Fig. 6d). Test results showed that the graphene STM tip is structurally stable, free of an oxide layer, and has 4000 times higher electrical conductivity than tungsten oxide tips, along with a longer lifespan. Hu et al.[97] used a Ni-based bimetallic catalyst to catalytically decompose acetylene under microwave irradiation at 400 °

C, producing hydrogen-rich gas products and forming CNTs. TEM analysis showed that the CNTs grown on the Ni–Pd-CNT catalyst exhibited good crystallinity and structural integrity (Fig. 6e).

Yi et al.[98] deposited graphitized carbon microspheres on cobalt nanosheets. The high aspect ratio improved the dielectric properties and enhanced electromagnetic wave absorption at low filler content. The composites achieved a minimum reflection loss of −65.7 dB and a reduction in radar cross-sectional area of 22.3 dB m^2 (Fig. 6f).

4.2 Microwaves in liquid reactions

Microwaves provide substantial benefits in liquid-phase reactions, such as rapid heating, shorter reaction times, higher yields and purity, and reduced solvent use, resulting in greener and more efficient processes.

Ma et al.[99] reported a facile, green, and novel method for the preparation of epoxy/graphene nanocomposites. In this method, epoxy resin was mixed with 4 wt% of graphite intercalation compound (GIC) particles (Fig. 7a). The mixture was then irradiated using a household microwave oven for 10 seconds, with the process repeated several times to maximize the expansion of the GIC, resulting in a total irradiation time of 30 minutes. Finally, the expanded GIC was exfoliated using the shear force of the mixer. In this method, the epoxy resin serves as both the exfoliation medium and the nanocomposite matrix. The resulting monolayer graphene was observed by TEM, and AFM measurements revealed that these graphene platelets have a thickness of 4.17 ± 0.63 nm and lateral dimensions of 1.00–4.77 μm (Fig. 7c). Additionally, a thin graphene film exhibited an electrical conductivity of 889 ± 141 S cm^{-1}.

Zhang et al.[100] utilized microwave-assisted synthesis to create Cu_3N/graphdiyne (GDY) catalysts (Fig. 7b). In this process, black graphene nanosheets were prepared via the Eglinton coupling reaction by mixing a hexaethynylbenzene monomer (HEB) with a previously prepared solution containing copper acetate. After that, the mixture was then processed in a household microwave oven for 2 minutes at 200 W of power. Transmission electron microscopy (Fig. 7d) and atomic force microscopy (Fig. 7e) images revealed the nanosheet structure of GDY, with a diameter of 15 μm and a thickness of 4.73 nm.

Chen et al.[101] used a microwave-assisted hydrothermal reaction to significantly improve reaction efficiency, producing reduced graphene oxide with a three-dimensional interconnected porous structure at 220 °C without a reducing agent in only 5 minutes. Compared to traditional chemical and thermal reduction methods, the microwave-reduced graphene oxide (MW-rGO) exhibits higher specific capacitance (298 F g^{-1}), better multiplicative performance and cycling stability, and an excellent energy storage performance of 25.0 W h kg^{-1} at a power density of 0.5 kW kg^{-1}. Wang et al.[102] obtained Fe and Ni bimetallic monatomic catalysts by dissolving $FeCl_3 \cdot 6H_2O$ and $Ni(NO_3)_2 \cdot 6H_2O$ in an ethylene glycol dispersion containing PNCH, treating them with 800 W microwaves for 20 minutes and then roasting them. These catalysts, used as air positive electrodes in zinc-air batteries, exhibited higher open circuit voltages and specific capacities than Pt/C cells.

Chen et al.[103] achieved the rapid and mild thermal reduction of graphene oxide (GO) to graphene using microwaves in a mixture of N,N-dimethylacetamide and water (DMAc/H_2O). They subjected both an aqueous suspension of GO (yellow-brown) and a mixture of GO and DMAc/H_2O to microwave treatment (800 W, 60 s). The aqueous GO solution showed no significant color change, while the GO/DMAc/H_2O mixture changed from yellow-brown to black, indicating reduction to graphene. The resulting graphene could be well dispersed in DMAc to form a stable organic suspension (Fig. 7f).
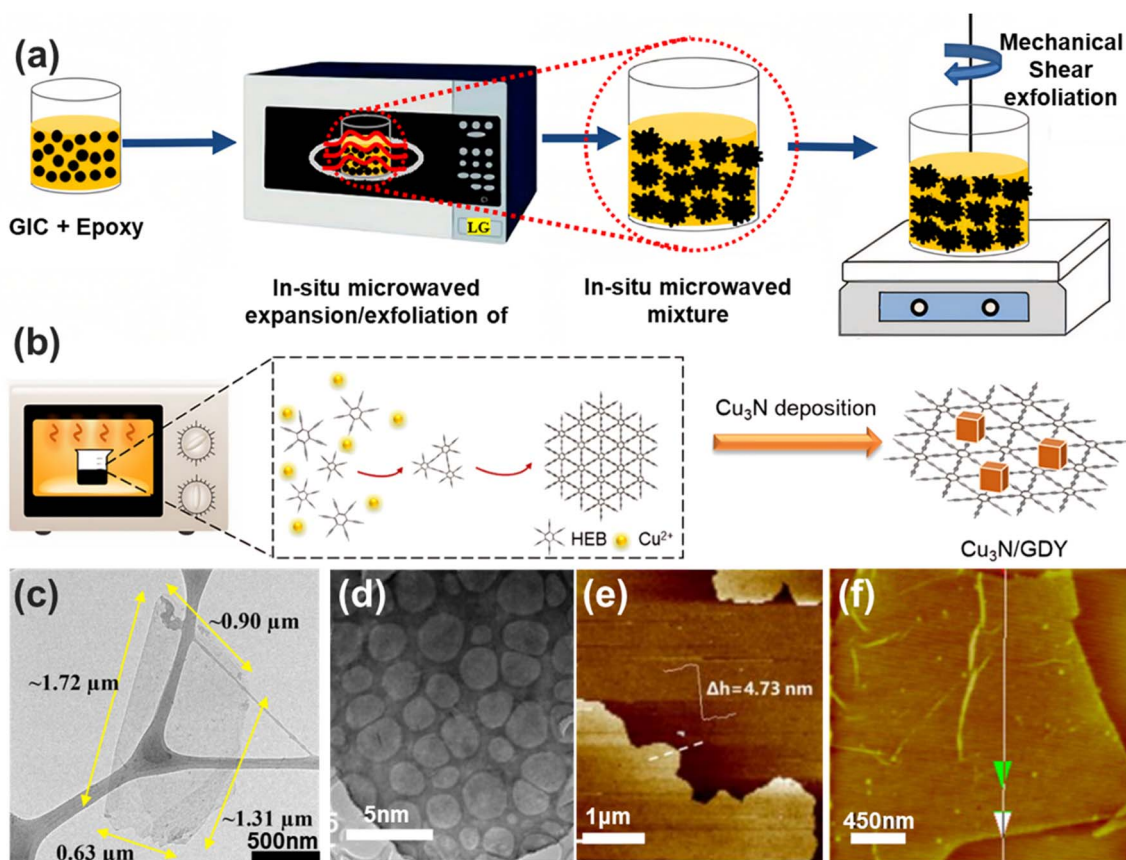

Fig. 7 (a) Schematic for preparation of epoxy/graphene nanocomposites. (b) Schematic illustration of the synthesis of Cu_3N/GDY. (c) TEM images of graphene platelets. (d) TEM and (e) AFM images of GDY. (f) Typical AFM height images of MW–rGO.

In addition to thermal effects, microwave plasma can transfer high-energy electrons and active radicals to the liquid through injection and diffusion during the reaction, facilitating the decomposition and reduction of catalysts in the liquid phase and enabling the preparation of composite carbon fibers, carbon nanomembranes, and other materials.[104,105]

Ferreira et al.[106] used microwave hydrothermal synthesis of carbon quantum dot transparent layers for UV protection. Microwave-assisted hydrothermal synthesis of carbon quantum dots took only 1 minute and yielded up to 55%. The coatings prepared by the microwave method showed more uniform absorbance and color compared to the oven-generated coatings, achieving superior UV absorbance and color gain. Studies have shown that the best coatings require more than 15 minutes of microwave treatment to filter 92% of UV light.

4.3 Microwaves in solid reactions

In solid-state reactions, microwaves act directly on the reactants, concentrating energy specifically on them. Solid materials generally have a high dielectric loss factor, which enables them to absorb microwave energy more efficiently and convert it into heat. This characteristic facilitates the attainment of high temperatures, making microwaves particularly advantageous for solid-state applications.

Zhou et al.[107] used active metal nanoparticles and microwave combustion to rapidly synthesize porous graphene with controllable pore sizes (Fig. 8a). They mixed 10 mL of a 3 mg mL^{-1} GO solution with varying amounts of silver acetate (0.2, 0.3, and 0.4 g), and the products obtained after ultrasonication and dehydration were treated with microwave radiation for 10 seconds. In this manner, porous graphene with pore sizes of approximately 5 nm, 30 nm, and 100 nm can be synthesized, while the specific surface area of the porous graphene with a pore size of 30 nm is as high as 965.64 m^2 g^{-1}. This method exploits the catalytic carbon oxidation mechanism of metal nanoparticles during rapid microwave heating and cooling to form the porous structure. The ion-selective membranes prepared from this porous graphene exhibit excellent performance, achieving a power density of about 1.15 W m^{-2} in salinity gradient power generation applications.

Zhang et al.[90] reported an efficient method for the microwave-assisted regeneration of single-walled carbon nanotubes (SWNTs) on Si/SO$_2$ substrates using carbon fragments. This method employs microwave irradiation to rapidly heat and
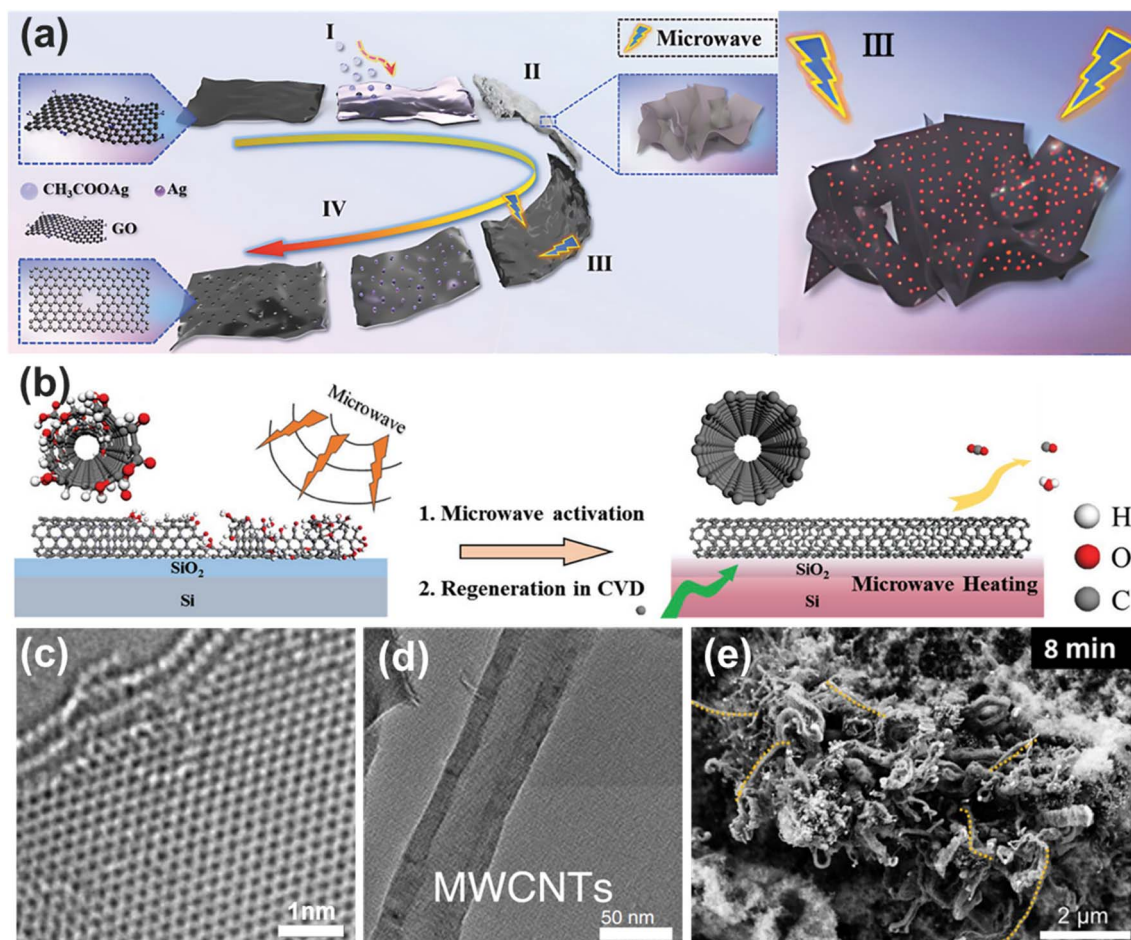

Fig. 8 (a) Schematic of the fabrication process for porous graphene. (b) Schematic showing the microwave-assisted regeneration of SWNTs. (c) HRTEM of MW-rGO showing a highly ordered structure. (d) Microwave-initiated catalytic deconstruction of plastic waste MWCNTs. (e) SEM image of the carbon product of plasma on Fe/activated carbon (AC) −400 for 8 minutes.

remove oxygen-containing groups from the carbon nanotubes, thereby reducing the spontaneous closure of their open ends. The surviving SWNTs and the attached carbon fragments, after plasma treatment, were simply microwaved and served as a template for regeneration. The schematic of this process is shown in Fig. 8b. The regenerated SWNTs were confirmed to retain the same chirality as the original SWNTs.

Voiry et al.[62] reported a method for the rapid reduction of graphene oxide (GO) to MW-rGO. This method is fast and efficient and significantly reduces energy loss compared to conventional thermal reduction methods. TEM images show that the structure of MW-rGO prepared using this method is highly ordered (Fig. 8c).

Using microwaves, waste can be processed in an environmentally friendly and pollution-free manner, transforming it into high-quality, value-added materials. Kim et al.[108] synthesized porous carbon with a graphite structure and high specific surface area from pretreated waste paper fibers in a single step using a 700 W microwave. The process simultaneously achieved carbonization and activation, producing porous carbon with a maximum specific capacitance of 237.7 F g^{-1} and a significant removal efficiency for various fuels, including a 95.0% removal efficiency for methylene blue. Edwards et al.[109] utilized a single-step microwave-initiated catalytic process to convert plastic waste mixed with an iron-based catalyst, rapidly heating the catalyst under microwave irradiation to initiate plastic catalytic decomposition, yielding a hydrogen-rich stream (up to 90 vol%) and primarily multiwalled carbon nanotubes (MWCNTs) as a carbonaceous residue (Fig. 8d). Zhang et al.[110] used an iron-based catalyst as a microwave inducer and employed metal tip-induced plasma discharge to significantly enhance hydrogen yield, achieving over 85% conversion efficiency and producing 300 mmol g^{-1} hydrogen, six times higher than that achieved by methods without plasma, while continuously producing high-value carbon nanotubes as a byproduct (Fig. 8e).

Besides well-known materials such as graphene and porous carbon, microwave-assisted synthesis has also been applied to other carbon-based materials. In recent years, fluorescent carbon nanoparticles (FCNPs) have been intensively studied and widely used due to their excellent optical properties, chemical stability and biocompatibility. Yang et al.[111] proposed a green and fast microwave-assisted solid-phase synthesis (solvent-free) method to prepare N-doped FCNPs using citric acid and aniline hydrochloride as carbon and nitrogen sources, respectively, without any solvent. The reaction took only 4 minutes, and the prepared FCNPs exhibited bright fluorescence in both aqueous and solid states with a quantum yield as high as 63.2%. The photoluminescence intensity of the FCNPs showed a sensitive pH response in the range of 3.47 to 5.10, and their potential for biological applications was verified by cell imaging experiments.

5. Conclusions and outlook

In this review, we summarize the mechanism of microwave action in the preparation of carbon-based materials and discuss in detail typical microwave reactors and preparation methods. The key conclusions can be summarized as follows:

(1) Microwave heating dynamics: microwave heating is characterized by its rapid temperature rise and selective heating properties. The temperature elevation of carbon-based materials involves converting microwave energy into thermal energy, primarily through dipole and dielectric losses. The intrinsic dielectric parameters of the material determine the efficiency of thermal conversion, the rate of temperature rise, and the uniformity of temperature distribution.

(2) Diversity in microwave reactors: the development of microwave reactors has become diversified. This ranges from simple modifications of domestic microwave ovens to sophisticated systems such as MPCVD and industrial microwave heating systems. These systems utilize various microwave excitation sources, resonance cavities, and auxiliary reactors, making them suitable for a wide range of material preparation applications.

(3) Applications in carbon-based materials: carbon-based materials can be used as microwave heating media, hotspots/arc plasma generators, and precursors for microwave-driven/assisted reactions, enabling rapid and efficient material fabrication.

Microwave technology, an emerging field, has experienced rapid advancements, offering advantages such as energy savings and operational efficiency. However, despite these advantages, significant technical bottlenecks still exist in practical applications. These limitations continue to hinder its further development and application in large-scale manufacturing. Future research efforts should focus on overcoming these challenges to fully exploit the potential of microwave technology:

(1) In practical reactions, the microwave absorption properties of carbon-based materials are influenced by various factors, including their composition, structure, and morphology, which can affect the electric field distribution and cause fluctuations in microwave intensity during the reaction. Given that these parameters are temperature-dependent and considering the black-box nature of microwave reactions, it is challenging for researchers to accurately assess energy consumption and intrinsic changes in reactants and products. This complexity makes it difficult to deduce the reaction mechanisms of microwave synthesis.

(2) Direct temperature measurement during microwave preparation remains a challenge due to hotspots caused by the absorption of carbon-based materials, the super-thermal effect of microwave-excited plasma, and the requirements for safe containment of the microwave reactor. For precise monitoring and control of microwave processes, specialized linear infrared thermometers or fiber-optic sensors can be used to measure macroscopic reaction temperatures with relative accuracy. Optical emission spectroscopy can be employed to collect optical signals that accompany the temperature rise in the reaction. By analyzing these signals, the electron temperature in the reaction can be calculated. Combining these measurements with theoretical calculations can help address this issue.

(3) The design of a microwave reactor, whether as a whole unit or as a modular component of a process plant, is crucial. Microwave processing often necessitates large-scale production, but scaling up experimental reactors is not straightforward. Sharp changes in microwave modes, field distributions, and electromagnetic field strength can significantly affect the quality and reproducibility of carbon material preparation.

(4) Due to the rapid response of microwave experiments, microwave radiation leaks are not as easily detected by experimenters as conventional hazards. High-power microwave radiation poses a serious health risk, necessitating the implementation of radiation protection measures in microwave experiments. Strict safety precautions must be followed when using microwave reactors to ensure both the safety and effectiveness of experiments.

We expect that this review will serve as a valuable resource for emerging researchers in the interdisciplinary field of microwave applications in carbon-based material preparation, providing critical insights and foundational knowledge.

Data availability

No new data were generated or analyzed in the course of this study. This review is based on previously published data, which are fully cited in the manuscript.

Conflicts of interest

There are no conflicts to declare.

Acknowledgements

References

1 T.-H. Han, H. Kim, S.-J. Kwon and T.-W. Lee, *Mater. Sci. Eng., R*, 2017, **118**, 1–43.

2 L. Ji, P. Meduri, V. Agubra, X. Xiao and M. Alcoutlabi, *Adv. Energy Mater.*, 2016, **6**, 1502159.

3 D. Deng, K. Novoselov, Q. Fu, N. Zheng, Z. Tian and X. Bao, *Nat. Nanotechnol.*, 2016, **11**, 218–230.

4 H. Zhang, G. Gruener and Y. Zhao, *J. Mater. Chem. B*, 2013, **1**, 2542–2567.

5 F. O. Perreault, A. F. De Faria and M. Elimelech, *Chem. Soc. Rev.*, 2015, **44**, 5861–5896.

6 K. S. Novoselov, L. Colombo, P. Gellert, M. Schwab and K. Kim, *Nature*, 2012, **490**, 192–200.

7 M.-M. Titirici, R. J. White, N. Brun, V. L. Budarin, D. S. Su, F. Del Monte, J. H. Clark and M. J. MacLachlan, *Chem. Soc. Rev.*, 2015, **44**, 250–290.

8 L. Zong, S. Zhou, N. Sgriccia, M. Hawley and L. Kempel, *J. Microwave Power*, 2003, **38**, 49–74.

9 M. Gupta and E. W. W. Leong, *Microwaves and Metals*, John Wiley & Sons, 2008.

10 M. Bhattacharya and T. Basak, *Energy*, 2016, **97**, 306–338.

11 M. Green and X. Chen, *J. Materiomics*, 2019, **5**, 503–541.

12 E. Thostenson and T.-W. Chou, *Composites, Part A*, 1999, **30**, 1055–1071.

13 A. M. Schwenke, S. Hoeppener and U. S. Schubert, *Adv. Mater.*, 2015, **27**, 4113–4141.

14 H. Bashiri, S. Nesari and M. Sarabadan, *Korean J. Chem. Eng.*, 2020, **37**, 240–248.

15 D. Aussems, K. Bystrov, İ. Doğan, C. Arnas, M. Cabié, T. Neisius, M. Rasiński, E. Zoethout, P. Lipman and M. van de Sanden, *Carbon*, 2017, **124**, 403–414.

16 R. Nagahata and K. Takeuchi, *Chem. Rec.*, 2019, **19**, 51–64.

17 Y. Li, N. Li, J. Zhou and Q. Cheng, *Compos. Struct.*, 2019, **212**, 83–93.

18 Z. Liu, K. Chen, R. Li, W. Li, M. Gong, X. Liu, W. Xia and D. Liu, *J. Anal. Appl. Pyrolysis*, 2024, **183**, 106785.

19 H. Y. Cho, A. Ajaz, D. Himali, P. A. Waske and R. P. Johnson, *J. Org. Chem.*, 2009, **74**, 4137–4142.

20 Y. Wang, H. Cao, C. Chen, Y. Xie, H. Sun, X. Duan and S. Wang, *Chem. Eng. J.*, 2019, **355**, 118–129.

21 F. Cameli, C. Xiouras and G. D. Stefanidis, *CrystEngComm*, 2018, **20**, 2897–2901.

22 L. Guo, L. Li, M. Liu, Q. Wan, J. Tian, Q. Huang, Y. Wen, S. Liang, X. Zhang and Y. Wei, *Mater. Sci. Eng., C*, 2018, **84**, 60–66.

23 M. Kallumottakkal, M. I. Hussein and M. Z. Iqbal, *Front. Mater.*, 2021, **8**, 633079.

24 D. Stuerga, *Microwaves in Organic Synthesis*, 2006, pp. 1–61.

25 D. Li, D. Jia, Z. Yang and Y. Zhou, *Int. Mater. Rev.*, 2022, **67**, 266–297.

26 Z. Wang, C. Yu, H. Huang, W. Guo, J. Yu and J. Qiu, *Nano Energy*, 2021, **85**, 106027.

27 R. R. Mishra and A. K. Sharma, *Composites, Part A*, 2016, **81**, 78–97.

28 B. Ashley, P. N. Vakil, B. B. Lynch, C. M. Dyer, J. B. Tracy, J. Owens and G. F. Strouse, *ACS Nano*, 2017, **11**, 9957–9967.

29 D. E. Clark, D. C. Folz and J. K. West, *Mater. Sci. Eng., A*, 2000, **287**, 153–158.

30 R. S. Rao, *Microwave Engineering*, PHI Learning Pvt. Ltd., 2015.

31 A. J. Moulson and J. M. Herbert, *Electroceramics: Materials, Properties, Applications*, John Wiley & Sons, 2003.

32 E. Grant and B. J. Halstead, *Chem. Soc. Rev.*, 1998, **27**, 213–224.

33 T. Auksornsri, J. Tang, Z. Tang, H. Lin and S. Songsermpong, *Innovative Food Sci. Emerging Technol.*, 2018, **45**, 98–105.

34 D. C. Campos, E. L. Dall'Oglio, P. T. de Sousa Jr, L. G. Vasconcelos and C. A. Kuhnen, *Fuel*, 2014, **117**, 957–965.

35 A. Gregory and R. Clarke, *Meas. Sci. Technol.*, 2007, **18**, 1372.

36 P. Debye, *Polar Molecules*, 1929.

37 R. Clarke, A. P. Gregory, D. Cannell, M. Patrick, S. Wylie, I. Youngs and G. Hill, *A guide to the characterisation of dielectric materials at RF and microwave frequencies*, Institute of Measurement and Control/National Physical Laboratory, 2003, **http://eprintspublications.npl.co.uk/id/eprint/2905**.

38 A. P. Gregory and R. Clarke, Tables of the complex permittivity of dielectric reference liquids at frequencies up to 5 GHz, 2012, **http://eprintspublications.npl.co.uk/id/eprint/4347**.

39 R. Sanjinés, M. D. Abad, C. Vâju, R. Smajda, M. Mionić and A. Magrez, *Surf. Coat. Technol.*, 2011, **206**, 727–733.

40 Y. Zhai, Y. Dou, D. Zhao, P. F. Fulvio, R. T. Mayes and S. Dai, *Adv. Mater.*, 2011, **23**, 4828–4850.

41 F. Siqueira and D. Campos, *Solid State Ionics*, 2023, **391**, 116140.

42 D. C. Campos, *J. Microwave Power*, 2020, **54**, 125–160.

43 B. Wang, Q. Wu, Y. Fu and T. Liu, *J. Mater. Sci. Technol.*, 2021, **86**, 91–109.

44 S. Gao, S.-H. Yang, H.-Y. Wang, G.-S. Wang and P.-G. Yin, *Carbon*, 2020, **162**, 438–444.

45 S. Qiu, H. Lyu, J. Liu, Y. Liu, N. Wu and W. Liu, *ACS Appl. Mater. Interfaces*, 2016, **8**, 20258–20266.

46 X. Zhang and D. O. Hayward, *Inorg. Chim. Acta*, 2006, **359**, 3421–3433.

47 X. Fan, B. Li, W. Zi, M. Kang, H. Wu, J. Bian and M. Sun, *Energy Convers. Manage.*, 2024, **301**, 118075.

48 Q. Li, Z. Zhang, L. Qi, Q. Liao, Z. Kang and Y. Zhang, *Adv. Sci.*, 2019, **6**, 1801057.

49 W. B. Thompson, *An Introduction to Plasma Physics*, Elsevier, 2013.

50 M. Mehdizadeh, *Microwave/RF Applicators and Probes: for Material Heating, Sensing, and Plasma Generation*, William Andrew, 2015.

51 V. Rybkin and D. Shutov, *Plasma Phys. Rep.*, 2017, **43**, 1089–1113.

52 A. Bogaerts and E. C. Neyts, *ACS Energy Lett.*, 2018, **3**, 1013–1027.

53 L. Bardos and H. Barankova, *Vacuum*, 2008, **83**, 522–527.

54 G. Kothandam, G. Singh, X. Guan, J. M. Lee, K. Ramadass, S. Joseph, M. Benzigar, A. Karakoti, J. Yi and P. Kumar, *Adv. Sci.*, 2023, **10**, 2301045.

55 M. A. Zafar and M. V. Jacob, *Rev. Modern Plasma Phys.*, 2022, **6**, 37.

56 S. Dąbrowska, T. Chudoba, J. Wojnarowicz and W. Łojkowski, *Crystals*, 2018, **8**, 379.

57 S. Horikoshi, R. F. Schiffmann, J. Fukushima and N. Serpone, *Microwave Chemical and Materials Processing*, 2018, pp. 33–45.

58 T. V. Chan and H. C. Reader, *Understanding microwave heating cavities*, Artech House, 2000, ISBN:158053094X.

59 J. Robinson, S. Kingman, D. Irvine, P. Licence, A. Smith, G. Dimitrakis, D. Obermayer and C. O. Kappe, *Phys. Chem. Chem. Phys.*, 2010, **12**, 4750–4758.

60 J. Asmussen, H. Lin, B. Manring and R. Fritz, *Rev. Sci. Instrum.*, 1987, **58**, 1477–1486.

61 R. Bajpai and D. Wagner, *Carbon*, 2015, **82**, 327–336.

62 D. Voiry, J. Yang, J. Kupferberg, R. Fullon, C. Lee, H. Y. Jeong, H. S. Shin and M. Chhowalla, *Science*, 2016, **353**, 1413–1416.

63 J. M. Kremsner and C. O. Kappe, *J. Org. Chem.*, 2006, **71**, 4651–4658.

64 C. Kappe, *Practical Microwave Synthesis for Organic Chemists: Strategies, Instruments, and Protocols*, Wiley-VCH, Verlag GmbH & Co. KGaA, 2009, ISBN:9783527320974, DOI: **10.1002/9783527623907**.

65 Y. Liu, Z. Ge, Z. Li and Y. Chen, *Nano Energy*, 2021, **80**, 105500.

66 M. B. Gawande, S. N. Shelke, R. Zboril and R. S. Varma, *Acc. Chem. Res.*, 2014, **47**, 1338–1348.

67 R. F. Gunnewiek, P. M. Souto and R. H. Kiminami, *J. Nanomater.*, 2017, **2017**, 3983468.

68 A. Mostofizadeh, Y. Li, B. Song and Y. Huang, *J. Nanomater.*, 2011, **2011**, 685081.

69 N. Bundaleska, D. Tsyganov, A. Dias, E. Felizardo, J. Henriques, F. Dias, M. Abrashev, J. Kissovski and E. Tatarova, *Phys. Chem. Chem. Phys.*, 2018, **20**, 13810–13824.

70 M. Santos, P. L. Michael, E. C. Filipe, A. H. Chan, J. Hung, R. P. Tan, B. S. Lee, M. Huynh, C. Hawkins and A. Waterhouse, *ACS Appl. Nano Mater.*, 2018, **1**, 580–594.

71 D. Tsyganov, N. Bundaleska, J. Henriques, E. Felizardo, A. Dias, M. Abrashev, J. Kissovski, A. Botelho do Rego, A. Ferraria and E. Tatarova, *Materials*, 2020, **13**, 4213.

72 C. Melero, R. Rincón, J. Muñoz, G. Zhang, S. Sun, A. Perez, O. Royuela, C. González-Gago and M. Calzada, *Plasma Phys. Controlled Fusion*, 2017, **60**, 014009.

73 Y. Sun, Z. Chen, H. Gong, X. Li, Z. Gao, S. Xu, X. Han, B. Han, X. Meng and J. Zhang, *Adv. Mater.*, 2020, **32**, 2002024.

74 Q. Wang, G. Wu, S. Liu, Z. Gan, B. Yang and J. Pan, *Crystals*, 2019, **9**, 320.

75 S. Zheng, G. Zhong, X. Wu, L. D'Arsiè and J. Robertson, *RSC Adv.*, 2017, **7**, 33185–33193.

76 J. Mammosser, S. Ahmed, K. Macha, J. Upadhyay, M. Nikolić and S. Popović, in *Proceedings Of the IPAC 2012*, 2012.

77 S. Altmannshofer, J. Boudaden, R. Wieland, I. Eisele and C. Kutter, *IOP Conf. Ser.:Mater. Sci. Eng.*, 2017, DOI: **10.1088/1757-899X/213/1/012021**.

78 X. Wei, W. Zhang, L. Chen, X. Xia, Y. Meng, C. Liu, Q. Lin, Y. Jiang and S. Gao, *Diamond Relat. Mater.*, 2022, **126**, 109094.

79 T. Yamada, M. Ishihara, J. Kim, M. Hasegawa and S. Iijima, *Carbon*, 2012, **50**, 2615–2619.

80 A. a. Metaxas and R. J. Meredith, *Industrial Microwave Heating*, IET, 1983.

81 G. D. Stefanidis, A. N. Munoz, G. S. Sturm and A. Stankiewicz, *Rev. Chem. Eng.*, 2014, **30**, 233–259.

82 Mitsui Chemicals, *Mitsui Chemicals Launches Microwave-Based Direct Monomerization Project for Plastic Waste*,

https://jp.mitsuichemicals.com/en/release/2021/
2021_1118/index.htm.

83 J. Zhang, V. S. Chevali, H. Wang and C.-H. Wang, *Composites, Part B*, 2020, **193**, 108053.

84 6K Inc., *6K is the world leader in creating, designing, and innovating Nano-Engineering Materials for Advanced Applications*, https://www.6kinc.com/applications/nano-engineered-powders/.

85 AMTek, *Advantages of Microwaves*, https://4amtek.com/advantages-of-microwaves/.

86 P. Fortugno, S. Musikhin, X. Shi, H. Wang, H. Wiggers and C. Schulz, *Carbon*, 2022, **186**, 560–573.

87 N. M. Mubarak, J. Sahu, R. R. Karri, E. Abdullah and M. Tripathi, *Int. J. Hydrogen Energy*, 2023, **48**, 21332–21344.

88 S. Dong, Y. Song, Y. Fang, K. Zhu, K. Ye, Y. Gao, J. Yan, G. Wang and D. Cao, *Carbon*, 2021, **178**, 1–9.

89 C. Yin, J. Li, T. Li, Y. Yu, Y. Kong, P. Gao, H. Peng, L. Tong and J. Zhang, *Adv. Funct. Mater.*, 2020, **30**, 2001396.

90 D. Lin, S. Zhang, Z. Zheng, W. Hu and J. Zhang, *Small*, 2018, **14**, 1800033.

91 J. Li, L. Lin, T. Ju, F. Meng, S. Han, K. Chen and J. Jiang, *Renewable Sustainable Energy Rev.*, 2024, **189**, 113979.

92 D. L. Tsyganov, N. Bundaleska and E. Tatarova, *Plasma Processes Polym.*, 2017, **14**, 1600161.

93 E. Tatarova, A. Dias, J. Henriques, M. Abrashev, N. Bundaleska, E. Kovacevic, N. Bundaleski, U. Cvelbar, E. Valcheva and B. Arnaudov, *Sci. Rep.*, 2017, **7**, 10175.

94 A. Dato, V. Radmilovic, Z. Lee, J. Phillips and M. Frenklach, *Nano Lett.*, 2008, **8**, 2012–2016.

95 Q. S. Zhenfei Gao, Z. Xiao, Z. Li, T. Li, J. Luo, S. Wang, W. Zhou, L. Li, J. Yu and J. Zhang, *Acta Phys. -Chim. Sin.*, 2023, **39**, 2307046.

96 S. Tang, Y. Zhang, Y. Tian, S. Jin, P. Zhao, F. Liu, R. Zhan, S. Deng, J. Chen and N. Xu, *Carbon*, 2017, **121**, 337–342.

97 S. Balyan, C. Jiang, A. Caiola and J. Hu, *Chem. Eng. J.*, 2023, **454**, 140115.

98 Q. Yi, F. Zhang, Y. Song, X. Wang, H. Zhang, C. Li and M. Piao, *Carbon*, 2023, **214**, 118322.

99 M. Naeem, H.-C. Kuan, A. Michelmore, S. Yu, A. P. Mouritz, S. S. Chelliah and J. Ma, *Carbon*, 2021, **177**, 271–281.

100 Z. Zhang, X. Feng, Z. Zhang, L. Chen, W. Liu, L. Tong, X. Gao and J. Zhang, *J. Am. Chem. Soc.*, 2024, 2307046.

101 A. R. Thiruppathi, J. van der Zalm, L. Zeng, M. Salverda, P. C. Wood and A. Chen, *J. Energy Storage*, 2022, **48**, 103962.

102 B. Wang, J. Tang, X. Zhang, M. Hong, H. Yang, X. Guo, S. Xue, C. Du, Z. Liu and J. Chen, *Chem. Eng. J.*, 2022, **437**, 135295.

103 W. Chen, L. Yan and P. R. Bangal, *Carbon*, 2010, **48**, 1146–1152.

104 Z. Zhong, C. Wang, R. Han, M. Gao, Y. Huang and S. Ramakrishna, *Compos. Commun.*, 2023, **38**, 101495.

105 A. M. Schwenke, S. Stumpf, S. Hoeppener and U. S. Schubert, *Adv. Funct. Mater.*, 2014, **24**, 1602–1608.

106 M. R. Silva, M. F. Alves, D. Ananias, M. Ivanov, M. H. V. Fernandes, P. M. Vilarinho and P. Ferreira, *Appl. Surf. Sci.*, 2024, **669**, 160414.

107 J. Wan, L. Huang, J. Wu, L. Xiong, Z. Hu, H. Yu, T. Li and J. Zhou, *Adv. Funct. Mater.*, 2018, **28**, 1800382.

108 J. Y. Son, S. Choe, Y. J. Jang and H. Kim, *Chemosphere*, 2024, **355**, 141798.

109 X. Jie, W. Li, D. Slocombe, Y. Gao, I. Banerjee, S. Gonzalez-Cortes, B. Yao, H. AlMegren, S. Alshihri and J. Dilworth, *Nat. Catal.*, 2020, **3**, 902–912.

110 P. Zhang, C. Liang, M. Wu, X. Chen, D. Liu and J. Ma, *Energy Convers. Manage.*, 2022, **268**, 116017.

111 S. Yang, X. Chen, S. Liu, F. Wang and G. Ouyang, *Talanta*, 2018, **186**, 80–87.